Available on CMS information server

**CMS CR -2022/218**

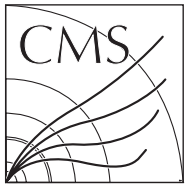

**The Compact Muon Solenoid Experiment**

**Conference Report**

Mailing address: CMS CERN, CH-1211 GENEVA 23, Switzerland

**04 November 2022 (v3, 21 November 2022)**

# RPC background studies at CMS experiment

Francesco Carnevali for the CMS Muon Group

**Abstract**

During Run2 the high instantaneous luminosity, up to $2.2 \cdot 10^{34}\ cm^{-2}\ s^{-1}$, lead to a substantial hit rate in the Compact Muon Solenoid experiment's muon chambers due to multiple background sources to physics processes sought for at LHC. In this article we will describe the analysis method devised to measure and identify the contributions to such background in the Resistive Plate Chambers.

Presented at *RPC2022 XVI Workshop of Resistive Plate Chamber and Related Detector at Cern in Sept. 2022*

# RPC background studies at CMS experiment

F. Carnevali[v], A. Samalan[a], M. Tytgat[a], M. El Sawy[b], G.A. Alves[c], F. Marujo[c], E.A. Coelho[c], E.M. Da Costa[d], H. Nogima[d], A. Santoro[d], S. Fonseca De Souza[d], D. De Jesus Damiao[d], M. Thiel[d], K. Mota Amarilo[d], M. Barroso Ferreira Filho[d], A. Aleksandrov[e], R. Hadjiiska[e], P. Iaydjiev[e], M. Rodozov[e], M. Shopova[e], G. Soultanov[e], A. Dimitrov[f], L. Litov[f], B. Pavlov[f], P. Petkov[f], A. Petrov[f], E. Shumka[f], S.J. Qian[g], H. Kou[h,i], Z.-A. Liu[h,i], J. Zhao[h,i], J. Song[h,i], Q. Hou[h,i], W. Diao[h,i], P. Cao[h,i], C. Avila[j], D. Barbosa[j], A. Cabrera[j], A. Florez[j], J. Fraga[j], J. Reyes[j], Y. Assran[k,l], M.A. Mahmoud[m], Y. Mohammed[m], I. Crotty[m], I. Laktineh[p], G. Grenier[p], M. Gouzevitch[p], L. Mirabito[p], K. Shchablo[p], I. Bagaturia[q], I. Lomidze[q], Z. Tsamalaidze[q], V. Amoozegar[r], B. Boghrati[r,s], M. Ebraimi[r], M. Mohammadi Najafabadi[r], E. Zareian[r], M. Abbrescia[t], G. Iaselli[t], G. Pugliese[t], P. Verwilligen[t], F. Loddo[t], N. De Filippis[t], R. Aly[t,o], D. Ramos[t], W. Elmetenawee[t], S. Leszki[t], I. Margjeka[t], D. Paesani[t], L. Benussi[u], S. Bianco[u], D. Piccolo[u], S. Meola[u], S. Buontempo[v], L. Lista[v], P. Paolucci[v], F. Fienga[w], A. Braghieri[x], P. Salvini[x], P. Montagna[y], C. Riccardi[y], P. Vitulo[y], E. Asilar[z], J. Choi[z], T.J. Kim[z], S.Y. Choi[aa], B. Hong[aa], K.S. Lee[aa], H.Y. Oh[aa], J. Goh[ab], I. Yu[ac], C. Uribe Estrada[ad], I. Pedraza[ad], H. Castilla-Valdez[ae], A. Sanchez-Hernandez[ae], R. L. Fernandez[ae], M. Ramirez-Garcia[af], E. Vazquez[af], M. A. Shah[af], N. Zaganidis[af], A. Radi[ag,n], H. Hoorani[ah], S. Muhammad[ah], A. Ahmad[ah], I. Asghar[ah], W.A. Khan[ah], J. Eysermans[ai], F. Torres Da Silva De Araujo[1], F. R. Cavallo[ak], H. Mei[al],
on behalf of the CMS Muon Group

[a] *Ghent University Dept. of Physics and Astronomy Proeftuinstraat 86 B-9000 Ghent Belgium.*
[b] *Universit Libre de Bruxelles Avenue Franklin Roosevelt 50-1050 Bruxelles Belgium.*
[c] *Centro Brasileiro Pesquisas Fisicas R. Dr. Xavier Sigaud 150 - Urca Rio de Janeiro - RJ 22290-180 Brazil.*
[d] *Dep. de Fisica Nuclear e Altas Energias Instituto de Fisica Universidade do Estado do Rio de Janeiro Rua Sao Francisco Xavier 524 BR - Rio de Janeiro 20559-900 RJ Brazil.*
[e] *Bulgarian Academy of Sciences Inst. for Nucl. Res. and Nucl. Energy Tzarigradsko shaussee Boulevard 72 BG-1784 Sofia Bulgaria.*
[f] *Faculty of Physics University of Sofia 5 James Bourchier Boulevard BG-1164 Sofia Bulgaria.*

*Email address:* francesco.carnevali@cern.ch (F. Carnevali)

[g]School of Physics Peking University Beijing 100871 China.
[h]State Key Laboratory of Particle Detection and Electronics Institute of High Energy Physics Chinese Academy of Sciences Beijing 100049 China.
[i]University of Chinese Academy of Sciences No.19(A) Yuquan Road Shijingshan District Beijing 100049 China.
[j]Universidad de Los Andes Carrera 1 no. 18A - 12 Bogot Colombia
[k]Egyptian Network for High Energy Physics Academy of Scientific Research and Technology 101 Kasr El-Einy St. Cairo Egypt.
[l]Suez University Elsalam City Suez - Cairo Road Suez 43522 Egypt.
[m]Center for High Energy Physics(CHEP-FU) Faculty of Science Fayoum University 63514 El-Fayoum Egypt.
[n]Department of Physics Faculty of Science Ain Shams University Cairo Egypt.
[o]Physics Department Faculty of Science Helwan University Ain Helwan 11795 Cairo Egypt.
[p]Univ Lyon Univ Claude Bernard Lyon 1 CNRS IN2P3 IP2I Lyon UMR 5822 F-69622 Villeurbanne France.
[q]Georgian Technical University 77 Kostava Str. Tbilisi 0175 Georgia.
[r]School of Particles and Accelerators Institute for Research in Fundamental Sciences (IPM) P.O. Box 19395-5531 Tehran Iran.
[s]School of Engineering Damghan University Damghan 3671641167 Iran.
[t]INFN Sezione di Bari Via Orabona 4 IT-70126 Bari Italy.
[u]INFN Laboratori Nazionali di Frascati (LNF) Via Enrico Fermi 40 IT-00044 Frascati Italy.
[v]INFN Sezione di Napoli Complesso Univ. Monte S. Angelo Via Cintia IT-80126 Napoli Italy.
[w]Dipartimento di Ingegneria Elettrica e delle Tecnologie dell'Informazione - Universit Degli Studi di Napoli Federico II IT-80126 Napoli Italy.
[x]INFN Sezione di Pavia Via Bassi 6 IT-Pavia Italy.
[y]INFN Sezione di Pavia and University of Pavia Via Bassi 6 IT-Pavia Italy.
[z]Hanyang University 222 Wangsimni-ro Sageun-dong Seongdong-gu Seoul Republic of Korea.
[aa]Korea University Department of Physics 145 Anam-ro Seongbuk-gu Seoul 02841 Republic of Korea.
[ab]Kyung Hee University 26 Kyungheedae-ro Dongdaemun-gu Seoul 02447 Republic of Korea.
[ac]Sungkyunkwan University 2066 Seobu-ro Jangan-gu Suwon Gyeonggi-do 16419 Republic of Korea.
[ad]Benemerita Universidad Autonoma de Puebla Puebla Mexico.
[ae]Cinvestav Av. Instituto Politcnico Nacional No. 2508 Colonia San Pedro Zacatenco CP 07360 Ciudad de Mexico D.F. Mexico.
[af]Universidad Iberoamericana Mexico City Mexico.
[ag]Sultan Qaboos University Al Khoudh Muscat 123 Oman.
[ah]National Centre for Physics Quaid-i-Azam University Islamabad Pakistan.
[ai]Massachusetts Institute of Technology 77 Massachusetts Ave Cambridge MA 02139 United States.

[aj] *III. Physikalisches Institut (A) RWTH Aachen University Sommerfeldstrasse D-52056 Aachen Germany.*
[ak] *INFN Sezione di Bologna Via B. Pichat 6 IT-Bologna Italy.*
[al] *Department of Physics University of Florida Gainesville FL 32611 United States.*

**Abstract**

During Run2 the high instantaneous luminosity, up to $2.2 \cdot 10^{34}\ cm^{-2}\ s^{-1}$, lead to a substantial hit rate in the Compact Muon Solenoid experiment's muon chambers due to multiple background sources to physics processes sought for at LHC. In this article we will describe the analysis method devised to measure and identify the contributions to such background in the Resistive Plate Chambers.Thorough understanding of the background rates provides the base for the upgrade of the muon detectors for the High-Luminosity LHC.

*Keywords:* CMS, RPC, LHC, Background, Muon System

PACS: 0000, 1111

2000 MSC: 0000,1111

## 1. The Compact Muon Solenoid Experiment

The Compact Muon Solenoid (CMS) is a general purpose experiment to explore the physics of the TeV scale in proton-proton collisions provided by the CERN Large Hadron Collider (LHC). The centre-of-mass energy $\sqrt{s}$ is equal to 13 TeV during the Run2 data taking, i.e. 2016-2018, and to 13.6 TeV during the Run3, started in 2022. It is made up of different subdetectors in order to detect particles and to reconstruct objects, featuring a superconducting solenoid that generates an approximately uniform magnetic field of 3.8 T, and an field of approximately 1.8 T in the CMS detection volume outside the solenoid. Muons constitute an important signature of new physics and their detection, triggering, reconstruction and identification

at CMS experiment is guaranteed by various sub-detectors. Fig. 1 shows a schematic view of the muon system: Drift Tubes and Resistive Plate Chambers (RPC) in the central region (barrel) and Cathode Strip Chambers, Gas Electron Multiplier (GEM), and RPC in the forward region (endcap). GEM detectors have been installed after Run2.

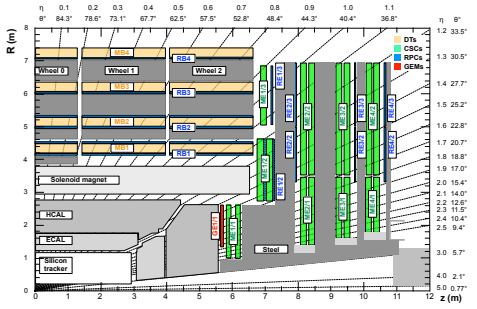


Figure 1: CMS Muon System schematic view. (1) (2)

### *1.1. Resistive Plate Chambers at CMS*

RPCs are double-gap chambers with Bakelite plates operating in avalanche mode with an intrinsic time resolution of $\approx 2$ ns. The latter is much less than the front-end electronic time window of 25 ns, allowing to assign the correct time slot of the detected particles and they are mostly used as trigger detectors both at the barrel and endcap (3). Chambers in the barrel are labelled as *RB* followed by number of station from 1, innermost station, i.e. closer to the beam, up to 4, outermost station. Chamber in the endcap are labelled as *RE* followed by the number of the disk and the number of the ring. RPCs are installed up to $|\eta| < 1.9$, where $\eta$ is the pseudorapidity. Particles are detected as "cluster" of adjacent hit strips, referred as reconstructed hit in the detector.

## 2. Background Studies

The quality triggering, identification, and reconstruction of muons could be degraded by background particles in the muon system. Understanding and analysing the background is a key point for maintaining robust operation and future upgrade choices. The background is made up of long-lived background (neutron background in the CMS cavern) and of the promptly induced background in the collisions. The background rate is expected to increase with the instantaneous luminosity, since the number of simultaneous collisions increases. The analysis of data taken on 2018 (Run2) shows in Fig. 2 a linear trend of the background hit rate as a function of the instantaneous luminosity for two different regions as example.

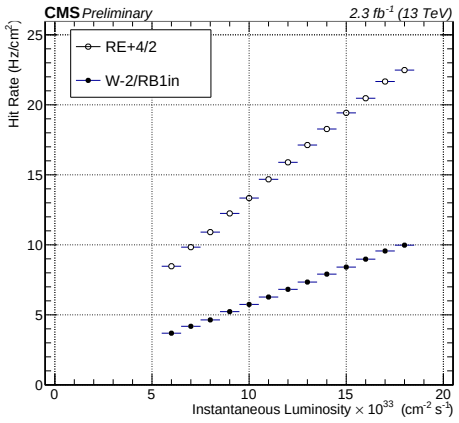


Figure 2: Background hit rate as a function of instantaneous luminosity for two different regions, the first layer of the innermost station of wheel -2 (W-2/RB1in) with full markers, and the second ring of the fourth positive endcap disk (RE+4/2). The rates show linear trends.

The data analyzed are enriched in background, which is dominated by the one measured during collisions, since the number of triggered events is much larger than the one with no collisions, and as such is influenced by the LHC filling scheme. One LHC orbit consists of 3564 units, said buckets, spaced 25 ns, and assigned an identification number each, called BX Id. The way those buckets are filled with a proton bunch or left vacant defines the filling scheme. The one adopted here has 48 consecutive colliding bunches, spaced by small or large gaps where there are not collisions (7 or 31-35 consecutive non-colliding bunches). The ensemble of all colliding BXs are referred to as *Colliding* region, to the *Non Colliding* region the whole of all gaps between two trains. The region before the first colliding bunch is labelled as *Pre-Beam* region, and the one after the last colliding bunch as *AbortGap* region. Fig. 3 shows the rate as function of BX Id for the W-2/RB1in region at fixed valued of $1.0 \cdot 10^{34}\ cm^{-2}\ s^{-1}$ of instantaneous luminosity, the shaded area indicates positions along the LHC orbit without collisions and it shows lower rates as expected.

The rate trend as function of instantaneous luminosity is studied separately for the four region of the filling scheme, i.e. *Colliding (C)*, *Non Colliding (NC)*, *Pre-Beam (PB)*, and *AbortGap (AG)* region. It is possible to define the inclusive (or total) background as:

$$B_{Tot} = \frac{N_C B_C + N_{NC} B_{NC} + N_{PB} B_{PB} + N_{AG} B_{AG}}{N_C + N_{NC} + N_{PB} + N_{AG}} \tag{1}$$

where B is the background measured and averaged in each region and N is the number of bunches of the region. The delayed (or secondary) background can be estimated as weighted average of the background measured in the three

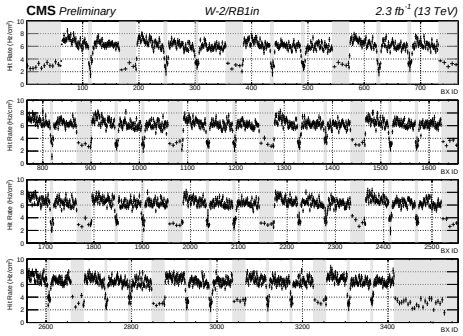


Figure 3: Background hit rate as function of BX Id for the W-2/RB1in region at fixed value of $1.0 \cdot 10^{34}$ $cm^{-2}$ $s^{-1}$ of instantaneous luminosity, the shaded area indicates positions along the LHC orbit without collisions.

regions with no collisions:

$$B_{Sec} = \frac{N_{NC}B_{NC} + N_{PB}B_{PB} + N_{AG}B_{AG}}{N_{NC} + N_{PB} + N_{AG}}. \quad (2)$$

The prompt (or primary) background can be estimated as the difference of the rate measured during collisions and the delayed background.

All rates are fitted as a linear function of the instantaneous luminosity, with the intercept representing the intrinsic RPC noise, and the results are shown in Fig. 4.

### *2.1. Background Rate vs η*

In order to have a clear overview of the rate in different detector regions, the background rate is evaluated as a function of $\eta$ at fixed value of $1.0 \cdot 10^{34}$ $cm^{-2}$ $s^{-1}$ of instantaneous luminosity, extracted from a linear fit, as shown above.

Fig. 5 shows the total, prompt, and delayed in the barrel region. The three rates increase with $|\eta|$. The prompt rate decrease with the increasing of R, i.e.

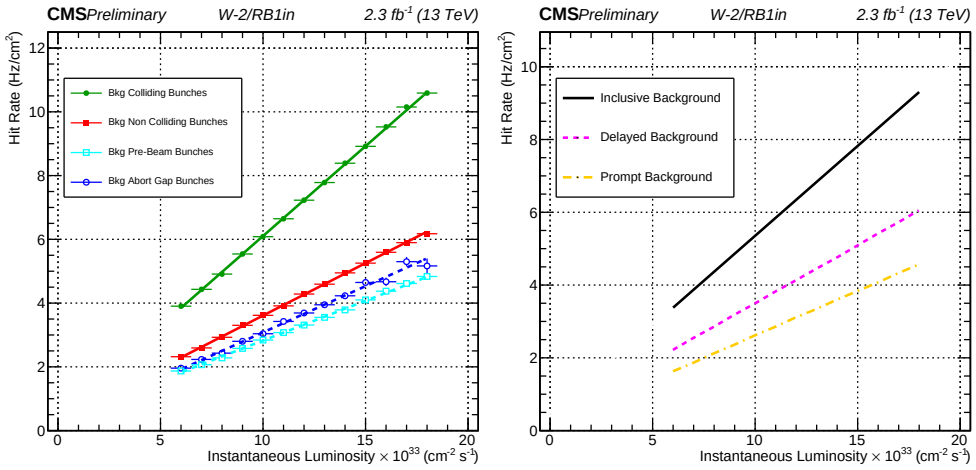


Figure 4: Background hit rate as function of instantaneous luminosity for the W-2/RB1in region in the four different filling scheme regions (left). Inclusive, delayed, and prompt background hit rate (right).

the distance of the chambers to the beam axis, in the outermost region the delayed background dominates, associated to the slow neutron background of the cavern, thus the delayed and total rate distributions are overlayed.

Fig. 6 shows the total, prompt, and delayed background rate in the endcap region, averaged between the positive and negative region. The prompt rate increases with the increasing of $|\eta|$, while the delayed background rate shows an initial decreasing and a consecutive increasing.

### *2.2. Run3 Results*

The background studies have been performed on Run3 data, taken on August 2022, at $\sqrt{s} = 13.6\ TeV$. The first results have been compared to the previous ones on Run2. Fig. 7 shows the background rate as a function of instantaneous luminosity for the Wheel+1 outermost region (W+1/RB4). As for this study the filling scheme is not taken into account and the colliding

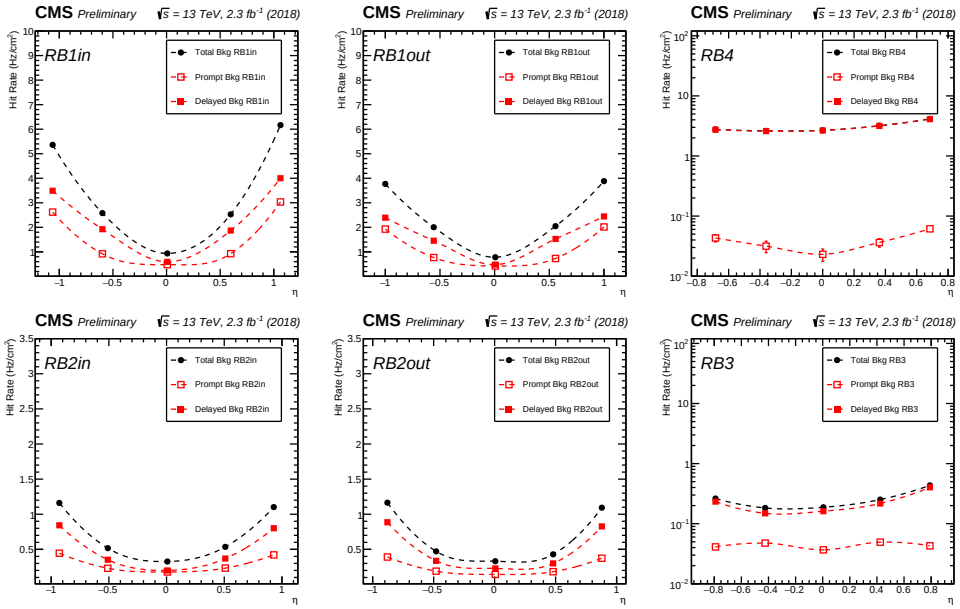


Figure 5: Total, prompt, and delayed background hit rate as function $\eta$ at fixed value of $1.0 \cdot 10^{34}\ cm^{-2}\ s^{-1}$ instantaneous luminosity for the barrel. In the RB4 region the total background rate is dominated by the delayed component and the two distributions are overlayed.

rate dominates, the two filling scheme are slightly different, 2400 colliding bunches in 2022 w.r.t. 2544 colliding bunches in 2018. Multiple mitigation actions, the most prominent being the installation of a set of shields during the Long Shutdown 2 (2019-2022), show a significant reduction of background in the outermost barrel region, improving the longevity and stability of the chambers.

## 3. Conclusions

Understanding the background is a key point for maintaining robust operation and for future upgrade choices. This study allowed to quantify the

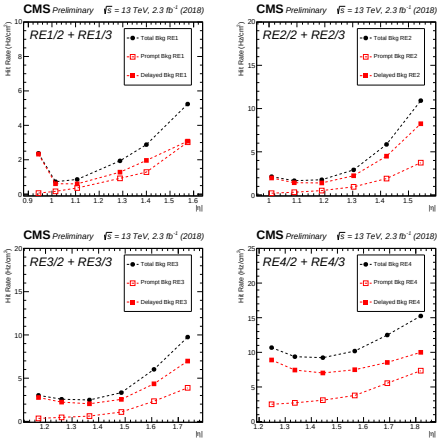


Figure 6: Total, prompt, and delayed background hit rate as function of $|\eta|$ at fixed value of $1.0 \cdot 10^{34}\ cm^{-2}\ s^{-1}$ instantaneous luminosity averaged for the positive and negative endcap regions.

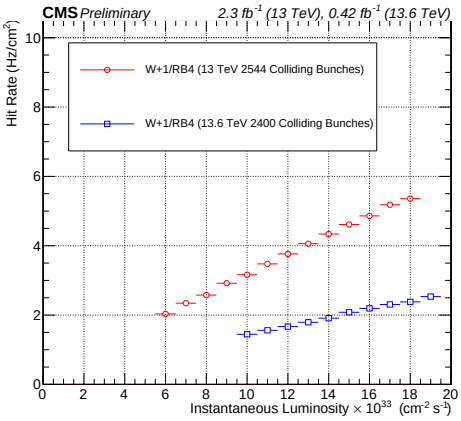


Figure 7: Background hit rate as a function of instantaneous luminosity for W+1/RB4 region. Run2 measured rate (red) is higher than Run3 measured one (blue).

increase of background rate as function of instantaneous luminosity, as well as the effect of the LHC filling scheme, and allowed to separate different components of the background: prompt, delayed, and total. Prompt background

rate increases with the decreasing of the distance to the beam in the barrel region and with the absolute value of $\eta$, while the delayed background rate dominates in the barrel outermost region. The effectiveness of background mitigation actions was tested, the most prominent being the installation of set of shields during the LS2, showing a significant reduction of background in the outermost barrel region, improving the longevity and stability of the chambers.

## References


[1] S. Chatrchyan, et al., The Performance of the CMS Muon Detector in Proton-Proton Collisions at $\sqrt{s} = 7$ TeV at the LHC, JINST 8 (2013) P11002. arXiv:1306.6905, doi:10.1088/1748-0221/8/11/P11002.

[2] M. Abbas, et al., Quality control of mass-produced GEM detectors for the CMS GE1/1 muon upgrade, Nucl. Instrum. Meth. A 1034 (2022) 166716. arXiv:2203.12037, doi:10.1016/j.nima.2022.166716.

[3] M. Abbrescia, et al., Beam test results on double-gap resistive plate chambers proposed for CMS experiment, Nucl. Instrum. Meth. A 414 (1998) 135–148. doi:10.1016/S0168-9002(98)00571-3.


## Acknowledgements


We congratulate our colleagues in the CERN accelerator departments for the excellent performance of the LHC and thank the technical and administrative staffs at CERN and at other CMS institutes for their contributions to the success of the CMS effort. In addition, we gratefully acknowledge the computing centres and personnel of the Worldwide LHC Computing Grid and other centres for delivering so effectively the computing infrastructure essential to our analyses. Finally, we acknowledge the enduring support for the construction and operation of the LHC, the CMS detector, and the supporting computing infrastructure provided by the following funding agencies: FWO (Belgium); CNPq, CAPES and FAPERJ (Brazil); MES

and BNSF (Bulgaria); CERN; CAS, MoST, and NSFC (China); MINCIENCIAS (Colombia); CEA and CNRS/IN2P3 (France); SRNSFG (Georgia); DAE and DST (India); IPM (Iran); INFN (Italy); MSIP and NRF (Republic of Korea); BUAP, CINVESTAV, CONACYT, LNS, SEP, and UASLP-FAI (Mexico); PAEC (Pakistan); DOE and NSF (USA).